

Quantum interference in a four-level system of a ^{87}Rb atom: Effects of spontaneously generated coherence

Dongsheng Wang* and Yujun Zheng†

School of Physics, Shandong University, Jinan 250100, China

(Dated: November 3, 2010)

In this work, the effects of quantum interference and spontaneously generated coherence (SGC) are theoretically analyzed in a four level system of a ^{87}Rb atom. For the effects of SGC, we find that a new kind of EIT channel can be induced due to destructive interference, and the nonlinear Kerr absorption can be coherently narrowed or eliminated under different strengths of the coupling and switching fields.

PACS numbers: 42.50.Gy, 42.65.Hw, 42.50.Ar

I. INTRODUCTION

The quantum interference and coherence play the central role in the fields of nonlinear optics, quantum information processing, and quantum wells/dots etc. In recent years, the processes of electromagnetically induced transparency (EIT) [1–9] are widely studied in various systems. Many processes based on EIT, for example, the electromagnetically induced absorption (EIA) [6], the EIT based four-wave and six-wave mixing [7], the EIT for X-rays [8], and the EIT on a single artificial atom [9] are studied. Also, the giant Kerr effect (GKE) [10–26] is the natural application of EIT by introducing the switching (signal) field, which has many applications, e.g., in the photonic Mott insulator [23] and the circuit quantum electrodynamics [24] etc. Physically, once the dark state within the EIT is destroyed by the disturbance of the switching field, the EIT disappears, the nonlinear susceptibility and absorptive photon switching occur. The processes of EIT and GKE could be changeable by turning the switching field on and off, and the photon process within can be managed. Recently, the effects of spontaneously generated coherence (SGC) (or termed as vacuum-induced coherence (VIC)) stimulate one's interests. For instance, in three-level systems the nonlinear Kerr absorptions are shown to be greatly enhanced via SGC [19]. For four-level system, the effects of SGC are studied in the N -type system [20] on the nonlinear Kerr absorption, and in double Λ -type system on the coherent population transfer [25, 26].

Experimentally, it is effective to simulate the effects of SGC by changing the property of the vacuum [27, 28], and/or extra driving fields, such as a dc field [29–31], a microwave field [32], or a laser field [33, 34] etc. Some experimental groups have realized part effects of SGC in the V -type, four-level Λ -type, and other systems recently [33–37].

In the present work we study the effects of SGC in EIT

and GKE in the four-level of N -type and double Λ -type systems based on the generating function approach developed recently [38–49]. In the double Λ -type system, SGC can cause new EIT channels due to destructive interference, which could be termed as “vacuum-assisted transparency” (VAT). The usual EIT requires that the detunings of the coupling and probe fields satisfy the two-photon resonance condition. With the effects of SGC, however, transparency can be obtained beyond the two-photon process. This means that we can get the transparency window within the whole detuning range of the probe field. For the nonlinear Kerr absorption in the N -type system, the spectra can be narrowed or eliminated with the effect of SGC, under different strengths of the coupling field Ω_c and switching field Ω_s . We demonstrate that the destroyed dark state can be repaired via SGC under some conditions. Also, we investigate the photon switching process via photon statistics, the variance of the photon distribution can be presented by Mandel's Q parameter. One of the important case is $Q < 0$, which shows anti-bunching when photon switching occurs.

For the four-level systems in this work, we demonstrate that SGC plays different roles in the linear and nonlinear absorption. By introducing SGC, the ability of the original EIT and GKE can be improved, also the photon statistics can be greatly affected and reflect the characters of different dynamics. The reasons we investigate two type systems together are as follows. Firstly, the two systems are, actually, the same with each other. They have the same structures, and a ^{87}Rb atom can be their concrete system. Secondly, the N -type and double Λ -type systems are apparent type, their difference comes from the numbers of driving laser fields.

SGC (VIC) shows us another pathway of quantum interference, which serves to mediate the relative contribution of the dipole transitions, and represents the directly coupling between the coherence of the system. SGC (VIC), represented by the generalized decay constants (GDCs), can lead to some novel features in dynamics of atomic systems, and it is shown that SGC plays the important role in many phenomenons [27–36, 50–64], such as the dark state resonance [51–53], coherent population trapping and transfer [54–57], spectral narrowing

*Electronic address: wdsn1987@gmail.com

†Electronic address: yzheng@sdu.edu.cn

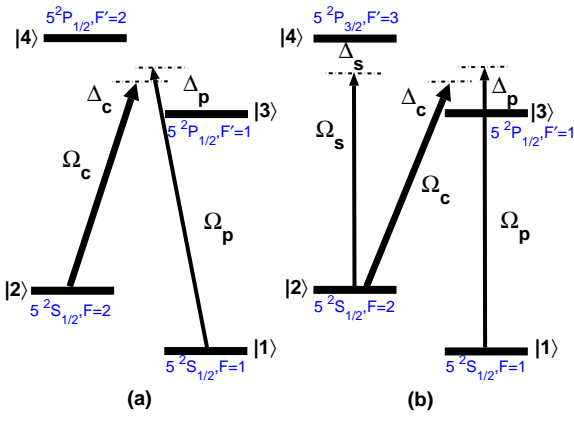


FIG. 1: (Color online) The schematic diagram of four-level system in this work. Panel (a) is double Λ -type, and panel (b) is N -type. The proposed D -line energy levels of the ^{87}Rb atom are marked on the diagram.

and elimination [58–60], gain without population inversion [61], spectrum squeezing [62–64] etc.

This paper is organized as follows. In Section II, we give our theoretical framework of the quantum dynamics of four-level system of a ^{87}Rb atom. In our theoretical framework, we include the generalized decay constants (GDCs) within the rotating wave approximation (RWA). In Section III, we present our theoretical results of the effect of SGC. In Section IV, we give brief conclusion and discussion.

II. THEORETICAL FRAMEWORK

In this work we theoretically study the quantum dynamics of a four-level quantum system driven by external laser fields. The four-level systems are shown in Fig. 1. In our study, we consider the transition dipole moments: $|3\rangle \rightarrow |1\rangle$, $|3\rangle \rightarrow |2\rangle$, $|4\rangle \rightarrow |1\rangle$, and $|4\rangle \rightarrow |2\rangle$. However the direct transitions between the states $|2\rangle$ and $|1\rangle$, and $|4\rangle$ and $|3\rangle$ are dipole forbidden. We consider the evolution of the reduced density matrix of the system $\sigma(t) \equiv \text{Tr}_R\{\rho(t)\}$. The evolution of the reduced density matrix satisfies the Liouville equation [65–68]

$$\dot{\sigma}_{ij}(t) = \mathcal{L}_{ij,kl} \sigma_{kl}, \quad (1)$$

where $\mathcal{L}_{ij,kl}$ is the Liouville super-operator. We study the effects of SGC on linear and nonlinear absorptions and also on the photon statistics. One of the convenient approach to calculate photon counting moments is generating function approach developed recently [38–49]. The generating function is defined as [38, 39]

$$\mathcal{G}(s,t) = \sum_{n=0}^{\infty} \sigma^{(n)}(t) s^n, \quad (2)$$

where s is called the counting variable, $\sigma^{(n)}(t)$ describes the probability that n photons have been emitted in the time interval $[0, t]$, and

$$\sigma(t) = \sum_{n=0}^{\infty} \sigma^{(n)}(t). \quad (3)$$

Similar with Refs. [38–49], the evolution of the generating function of four-level system can, under the rotating wave approximation (RWA), be formally written as

$$\begin{aligned} \dot{\mathcal{G}}_{ij}(s,t) &= -i\omega_{ij}\mathcal{G}_{ij} - i/2 \sum_m (\Omega_{mj}\mathcal{G}_{im} - \Omega_{im}\mathcal{G}_{mj}) \\ &\quad + 2s \sum_{k>i, l>j} \gamma_{kijl}\mathcal{G}_{kl} - \sum_{k>m} \gamma_{immk}\mathcal{G}_{kj} - \sum_{l>n} \gamma_{lnnj}\mathcal{G}_{il}, \end{aligned} \quad (4)$$

where the energy spacing $\omega_{ij} = \omega_i - \omega_j$, the Rabi frequency $\Omega_{ij}(t) = \omega_{ij} \cdot \mathcal{E}(t)/\hbar$, $\mathcal{E}(t)$ is the polarization of the field with frequency ω_L , the GDCs are $\gamma_{ijkl} = \mu_{ij} \cdot \mu_{kl} \frac{|\omega_{kl}|^3}{6\varepsilon_0 \hbar \pi c^3}$, where $\omega_{kl} \approx \omega_{ij}$ has been taken into account. $k > i$ represents that the level $|k\rangle$ sits above the level $|i\rangle$. Eq. (4) for the double Λ -type system and N -type system considered in this work is explicitly presented in the following section.

In our study, the GDCs γ_{ijkl} can be expressed as [25, 31, 61–64]

$$\gamma_{kiiil} = \beta \sqrt{\gamma_{kik}\gamma_{liil}}, \quad (5)$$

the parameter β could be named as the “SGC factor”, it takes $0 \leq \beta \leq 1$. When the dipole moments are perpendicular $\beta = 0$, and $\beta = 1$ for the dipole moments parallel case.

In order to extract the information of photon emission events, we define the working generating function

$$\mathcal{Y}(s,t) = \sum_{k=1}^4 \mathcal{G}_{kk}(s,t). \quad (6)$$

The factorial moments $\langle N^{(m)} \rangle(t)$ and emission probability of n photon $P_n(t)$ can be obtained via [38, 39]

$$\begin{aligned} \langle N^{(m)} \rangle(t) &= \langle N(N-1)(N-2) \cdots (N-m+1) \rangle(t) \\ &= \frac{\partial^m}{\partial s^m} \mathcal{Y}(s,t)|_{s=1}, \end{aligned} \quad (7)$$

and

$$P_n(t) = \frac{1}{n!} \frac{\partial^n}{\partial s^n} \mathcal{Y}(s,t)|_{s=0}. \quad (8)$$

Correspondingly, the absorption line shapes and Mandel's Q parameter can be obtained

$$I(\omega_L) = \frac{d}{dt} \langle N^{(1)} \rangle(t)|_{t \rightarrow \infty}, \quad (9)$$

$$Q(\omega_L) = \frac{\langle N^{(2)} \rangle - \langle N^{(1)} \rangle^2}{\langle N^{(1)} \rangle}. \quad (10)$$

III. NUMERICAL RESULTS

In this section, we study the effects of SGC on electromagnetically induced transparency and nonlinear Kerr absorption, and on the photon statistics. In our numerical results, we plot absorption line shapes and Mandel's Q parameter. The absorption is monitored via fluorescence of spontaneously emitted photons. The reason is that the correspondence between photon emission and absorption is insured by conservation of energy [42, 44]. Our results can be measured experimentally based on a ^{87}Rb atom. For the convenient of future experiment, all the parameters used in our numerical results are the parameters of the ^{87}Rb atom, the proposed D -line energy levels of the ^{87}Rb atom in this work are also marked in Fig. 1. In the following equations of generating function (12) and (13), for convenience, we use the shorthand

$$\begin{aligned} \gamma_{31} &\equiv \gamma_{3113}, \quad \gamma_{32} \equiv \gamma_{3223}, \\ \gamma_{41} &\equiv \gamma_{4114}, \quad \gamma_{42} \equiv \gamma_{4224}, \\ \gamma_{314} &\equiv \gamma_{3114}, \quad \gamma_{324} \equiv \gamma_{3224}, \\ \Gamma_3 &\equiv \gamma_{3113} + \gamma_{3223}, \\ \Gamma_4 &\equiv \gamma_{4114} + \gamma_{4224}, \\ \Gamma_{34} &\equiv \gamma_{3114} + \gamma_{3224}. \end{aligned} \quad (11)$$

It should be noted that we normalize the absorption line shapes in the following sections.

A. DOUBLE Λ -TYPE SYSTEM

In this subsection, we study the process of EIT in the double Λ -type system. Its schematic diagram is shown in panel (a) of Fig. 1. In our numerical results, we refer to the parameters of the ^{87}Rb atom, namely, we set $|5^2S_{1/2}, F = 1\rangle = |1\rangle$, $|5^2S_{1/2}, F = 2\rangle = |2\rangle$, $|5^2P_{1/2}, F' = 1\rangle = |3\rangle$, and $|5^2P_{1/2}, F' = 2\rangle = |4\rangle$. The parameters are listed in the caption of Fig. 2.

In this system, the transitions of $|3\rangle \rightarrow |1\rangle$ and $|4\rangle \rightarrow |1\rangle$ are probed by the weak probe field, the transitions of $|3\rangle \rightarrow |2\rangle$ and $|4\rangle \rightarrow |2\rangle$ are coupled by the strong coupling field. The Rabi frequencies are defined as $\Omega_{13} = \Omega_{14} = \Omega_p$, $\Omega_{23} = \Omega_{24} = \Omega_c$. The detunings are defined as $\Delta_p = \omega_p - \omega_{31}$, $\Delta_c = \omega_c - \omega_{32}$, and the separation of the excited states $\omega = \omega_4 - \omega_3$. The generating function of Eq. (4) for the double Λ -type system is obviously expressed as

$$\begin{aligned} \dot{\mathcal{G}}_{11} &= 2s(\gamma_{31}\mathcal{G}_{33} + \gamma_{314}\mathcal{G}_{34} + \gamma_{314}\mathcal{G}_{43} + \gamma_{41}\mathcal{G}_{44}) - \frac{i}{2}\Omega_p(\mathcal{G}_{13} + \mathcal{G}_{14} - \mathcal{G}_{31} - \mathcal{G}_{41}), \\ \dot{\mathcal{G}}_{22} &= 2(\gamma_{32}\mathcal{G}_{33} + \gamma_{324}\mathcal{G}_{34} + \gamma_{324}\mathcal{G}_{43} + \gamma_{42}\mathcal{G}_{44}) - \frac{i}{2}\Omega_c(\mathcal{G}_{23} + \mathcal{G}_{24} - \mathcal{G}_{32} - \mathcal{G}_{42}), \\ \dot{\mathcal{G}}_{33} &= -2\Gamma_3\mathcal{G}_{33} - \Gamma_{34}(\mathcal{G}_{34} + \mathcal{G}_{43}) - \frac{i}{2}\Omega_p(\mathcal{G}_{31} - \mathcal{G}_{13}) - \frac{i}{2}\Omega_c(\mathcal{G}_{32} - \mathcal{G}_{23}), \\ \dot{\mathcal{G}}_{44} &= -2\Gamma_4\mathcal{G}_{44} - \Gamma_{34}(\mathcal{G}_{34} + \mathcal{G}_{43}) - \frac{i}{2}\Omega_p(\mathcal{G}_{41} - \mathcal{G}_{14}) - \frac{i}{2}\Omega_c(\mathcal{G}_{42} - \mathcal{G}_{24}), \\ \dot{\mathcal{G}}_{12} &= -i(\Delta_p - \Delta_c)\mathcal{G}_{12} - \frac{i}{2}\Omega_c(\mathcal{G}_{13} + \mathcal{G}_{14}) + \frac{i}{2}\Omega_p(\mathcal{G}_{32} + \mathcal{G}_{42}), \\ \dot{\mathcal{G}}_{13} &= -i\Delta_p\mathcal{G}_{13} - \Gamma_3\mathcal{G}_{13} - \Gamma_{34}\mathcal{G}_{14} - \frac{i}{2}\Omega_p(\mathcal{G}_{11} - \mathcal{G}_{33} - \mathcal{G}_{43}) - \frac{i}{2}\Omega_c\mathcal{G}_{12}, \\ \dot{\mathcal{G}}_{14} &= -i(\Delta_p - \omega)\mathcal{G}_{14} - \Gamma_{34}\mathcal{G}_{13} - \Gamma_4\mathcal{G}_{14} - \frac{i}{2}\Omega_p(\mathcal{G}_{11} - \mathcal{G}_{34} - \mathcal{G}_{44}) - \frac{i}{2}\Omega_c\mathcal{G}_{12}, \\ \dot{\mathcal{G}}_{23} &= -i\Delta_c\mathcal{G}_{23} - \Gamma_3\mathcal{G}_{23} - \Gamma_{34}\mathcal{G}_{24} - \frac{i}{2}\Omega_c(\mathcal{G}_{22} - \mathcal{G}_{33} - \mathcal{G}_{43}) - \frac{i}{2}\Omega_p\mathcal{G}_{21}, \\ \dot{\mathcal{G}}_{24} &= -i(\Delta_c - \omega)\mathcal{G}_{24} - \Gamma_{34}\mathcal{G}_{23} - \Gamma_4\mathcal{G}_{24} - \frac{i}{2}\Omega_c(\mathcal{G}_{22} - \mathcal{G}_{34} - \mathcal{G}_{44}) - \frac{i}{2}\Omega_p\mathcal{G}_{21}, \\ \dot{\mathcal{G}}_{34} &= i\omega\mathcal{G}_{34} - \Gamma_{34}(\mathcal{G}_{33} + \mathcal{G}_{44}) - (\Gamma_3 + \Gamma_4)\mathcal{G}_{34} - \frac{i}{2}\Omega_p(\mathcal{G}_{31} - \mathcal{G}_{14}) - \frac{i}{2}\Omega_c(\mathcal{G}_{32} - \mathcal{G}_{24}), \end{aligned} \quad (12)$$

and the elements not included in Eq. (12) can be obtained by using the complex conjugate relation: $\mathcal{G}_{ij} = \mathcal{G}_{ji}^*$.

The EIT process in the detuning space Δ_p - Δ_c is shown in Fig. 2. Panels (a) and (b) are the results of the SGC factor $\beta = 0$, and panels (c) and (d) are the results of

$\beta = 1$. Panels (a) and (c) are absorption line shapes, and panels (b) and (d) are Mandel's Q_p parameters.

When $\beta = 0$, there is no effect of SGC. The absorption line shapes I_p of the probe field is shown in Fig. 2 (a). It can be seen the transparency signal is on the diagonal

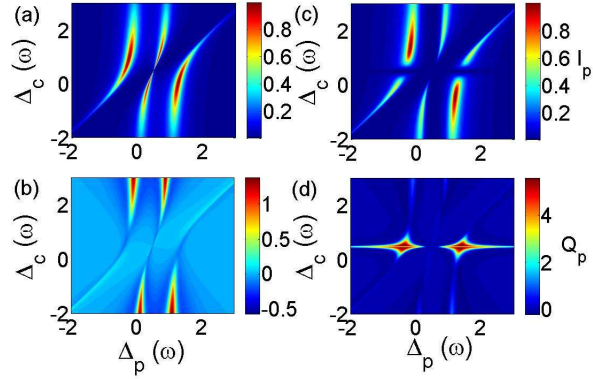


FIG. 2: (Color online) The absorption line shapes I_p (panels (a) and (c)) and Mandel's Q_p parameter (panels (b) and (d)) of the EIT of the double Λ -type system in the detuning space Δ_p - Δ_c . The parameters are used the same with the ^{87}Rb atom [13, 22, 71–73]: $\gamma_{31} = \gamma_{32} = \gamma_{41} = \gamma_{42} = 1.4375\text{MHz}$, $\omega = 814.5\text{MHz}$. The initial state is $|\psi\rangle = |1\rangle$. The other parameters are $\Omega_p = 0.1\omega$, $\Omega_c = \omega$, and $\gamma_{314} = \gamma_{324} = 0$ for $\beta = 0$ (panels (a) and (b)); $\gamma_{314} = \gamma_{324} = \sqrt{\gamma_{31}\gamma_{41}} = 1.4375\text{MHz}$ for $\beta = 1$ (panels (c) and (d)). In the study of double Λ -type system, the detunings (Δ_p , Δ_c) and Rabi frequencies (Ω_p , Ω_c) are in the units of ω .

$\Delta_p = \Delta_c$, corresponding to the two-photon absorption process. For fixed detuning Δ_c , there are usually three peaks of I_p as the function of Δ_p since two dark states are induced in this system. Particularly, when $\Delta_c = 0.5\omega$, the central peak vanishes as the EIT occurs. Part of the similar processes are studied experimentally in the ^{85}Rb atoms system [33] for particular coupling detunings Δ_c .

For the case of the SGC factor $\beta = 1$, the GDCs γ_{314} and γ_{324} cause new EIT process. From Fig. 2 (c), we can see the two new EIT channels along the Δ_p -axis for $\Delta_c = 0.5\omega$, and along the Δ_c -axis for $\Delta_p = 0.5\omega$ in absorption line shapes. Physically, the GDCs γ_{314} (γ_{324}) can cause destructive interference between the transitions $|3\rangle \rightarrow |1(2)\rangle$ and $|4\rangle \rightarrow |1(2)\rangle$ if the states $|3\rangle$ and $|4\rangle$ are equally excited. The dark state is induced as the destructive interference between states $|3\rangle$ and $|4\rangle$. This can also be viewed as the phenomenon of dark resonance [43, 49, 51].

These two new EIT processes are not the same with the usual EIT (the diagonal channel) because they are assisted by SGC. We name them as the “vacuum-assisted transparency” (VAT). Experimentally, for example, we can introduce another field Ω_0 between the excited states $|3\rangle$ and $|4\rangle$ to simulate the effects of SGC, the quantum system of the ^{87}Rb atom then seems to be “locked” by this field and the coupling field with $\Delta_c = 0.5\omega$, and the probe field can not disturb the ^{87}Rb atom and form the totally transparent window. Also, we can control the transparency window by whether turning the field Ω_0 on or by changing its strength.

To understand the dynamics in this process, as an example, we analyze the VAT channel along the Δ_p -axis

for $\Delta_c = 0.5\omega$. When $\Delta_c = 0.5\omega$, for any Δ_p there is no absorption of the probe field. The reason is that the population trapping happens. When the atom is excited (except when the detuning $\Delta_p = 0.5\omega$), the population ρ_{11} transfers to other three states, and they can not jump back to the ground state again due to influences of SGC. The trapping is controlled by the coupling field and GDCs. Specially, the populations ρ_{33} and ρ_{44} ($\rho_{33} = \rho_{44}$) are in proportion to the strengths of coupling field Ω_c , while the population ρ_{22} is in inverse proportion to Ω_c . The process for $\Delta_p = 0.5\omega$ is different since the usual EIT channel is induced. The population is almost trapped in the initial ground state ($|1\rangle$ in our calculation). The difference between the processes of EIT and VAT means that we can control the population transfer [57] by turning the detuning of the coupling field Δ_c . This process of population trapping is similar with the studies in Refs. [29, 30, 55]. In the four-level system in Refs. [29, 30, 55], two close-lying excited states couple to another auxiliary state by a driving field, and decay to the single ground state. In our system, the difference is that the coupling field and probe field can perform the EIT channel, we can combine the effects of EIT and SGC together, and switch between EIT ($\beta = 0$) and VAT ($\beta \neq 0$). In addition, if the coupling field is turned off, there will be no transparency even though SGC exists. That is to say, the coupling field is necessary to induce the VAT channel.

The characters of Q_p parameter are plotted in panels (b) and (d) of Fig. 2. As we know, when $Q > 0$, the behavior of photon statistics is bunching, and when $Q < 0$, the behavior of photon statistics is anti-bunching. In Fig. 2 (b), the Q_p parameter shows the standard transition between bunching and anti-bunching when absorption occurs [39, 41]. When $\beta = 1$, however, the photon statistics shows bunching effect. The fluctuation of photon emission is enhanced, especially for the two bright branches on the Q_p spectra as shown in Fig. 2 (d). This means that the natures of photon emission statistics can be greatly affected by SGC.

B. N-TYPE SYSTEM

In previous section we investigate the vacuum-assisted transparency. If we apply the switching field, the double Λ -type system becomes the N -type system. The schematic diagram of this N -type four-level system is shown in panel (b) of Fig. 1. We study the GKE in N -type four-level system in this subsection, and we compare with the experimental results of Ref. [12]. Some interesting properties, such as the photon switching, frequency conversion etc are investigated by employing this system [10–22]. It is shown that the process of photon emission is different with that in the double Λ system: the nonlinear Kerr absorption occurs while the stability of the dark state within the EIT is destroyed. With the effects of SGC, however, the destroyed dark state can be

repaired under some conditions.

For this system, based on the ^{87}Rb atom, we set the states as $|5^2S_{1/2}, F = 1\rangle = |1\rangle$, $|5^2S_{1/2}, F = 2\rangle = |2\rangle$, $|5^2P_{1/2}, F' = 1\rangle = |3\rangle$, and $|5^2P_{3/2}, F' = 3\rangle = |4\rangle$. The weak probe field is set on transition $|3\rangle \rightarrow |1\rangle$, the strong coupling field is set on transition $|3\rangle \rightarrow |2\rangle$, the third

switching field is set on transition $|4\rangle \rightarrow |2\rangle$. The Rabi frequencies are noted as $\Omega_{13} = \Omega_p$, $\Omega_{23} = \Omega_c$, $\Omega_{24} = \Omega_s$. The detuning frequencies are defined as $\Delta_p = \omega_p - \omega_{31}$, $\Delta_c = \omega_c - \omega_{32}$, $\Delta_s = \omega_s - \omega_{42}$. After these preparations, the equations of generating function of Eq. (4) for the N -type system are written as follows

$$\begin{aligned}\dot{\mathcal{G}}_{11} &= 2s(\gamma_{31}\mathcal{G}_{33} + \gamma_{314}\mathcal{G}_{34} + \gamma_{314}\mathcal{G}_{43} + \gamma_{41}\mathcal{G}_{44}) - \frac{i}{2}\Omega_p(\mathcal{G}_{13} - \mathcal{G}_{31}), \\ \dot{\mathcal{G}}_{22} &= 2(\gamma_{32}\mathcal{G}_{33} + \gamma_{324}\mathcal{G}_{34} + \gamma_{324}\mathcal{G}_{43} + \gamma_{42}\mathcal{G}_{44}) - \frac{i}{2}\Omega_c(\mathcal{G}_{23} - \mathcal{G}_{32}) - \frac{i}{2}\Omega_s(\mathcal{G}_{24} - \mathcal{G}_{42}), \\ \dot{\mathcal{G}}_{33} &= -2\Gamma_3\mathcal{G}_{33} - \Gamma_{34}(\mathcal{G}_{34} + \mathcal{G}_{43}) - \frac{i}{2}\Omega_p(\mathcal{G}_{31} - \mathcal{G}_{13}) - \frac{i}{2}\Omega_c(\mathcal{G}_{32} - \mathcal{G}_{23}), \\ \dot{\mathcal{G}}_{44} &= -2\Gamma_4\mathcal{G}_{44} - \Gamma_{34}(\mathcal{G}_{34} + \mathcal{G}_{43}) - \frac{i}{2}\Omega_s(\mathcal{G}_{42} - \mathcal{G}_{24}), \\ \dot{\mathcal{G}}_{12} &= -i(\Delta_p - \Delta_c)\mathcal{G}_{12} - \frac{i}{2}(\Omega_c\mathcal{G}_{13} + \Omega_s\mathcal{G}_{14} - \Omega_p\mathcal{G}_{32}), \\ \dot{\mathcal{G}}_{13} &= -i\Delta_p\mathcal{G}_{13} - \Gamma_3\mathcal{G}_{13} - \Gamma_{34}\mathcal{G}_{14} - \frac{i}{2}\Omega_p(\mathcal{G}_{11} - \mathcal{G}_{33}) - \frac{i}{2}\Omega_c\mathcal{G}_{12}, \\ \dot{\mathcal{G}}_{14} &= -i(\Delta_p - \Delta_c + \Delta_s)\mathcal{G}_{14} - \Gamma_{34}\mathcal{G}_{13} - \Gamma_4\mathcal{G}_{14} - \frac{i}{2}(\Omega_s\mathcal{G}_{12} - \Omega_p\mathcal{G}_{34}), \\ \dot{\mathcal{G}}_{23} &= -i\Delta_c\mathcal{G}_{23} - \Gamma_3\mathcal{G}_{23} - \Gamma_{34}\mathcal{G}_{24} - \frac{i}{2}\Omega_c(\mathcal{G}_{22} - \mathcal{G}_{33}) - \frac{i}{2}(\Omega_p\mathcal{G}_{21} - \Omega_s\mathcal{G}_{43}), \\ \dot{\mathcal{G}}_{24} &= -i\Delta_s\mathcal{G}_{24} - \Gamma_{34}\mathcal{G}_{23} - \Gamma_4\mathcal{G}_{24} - \frac{i}{2}\Omega_s(\mathcal{G}_{22} - \mathcal{G}_{44}) + \frac{i}{2}\Omega_c\mathcal{G}_{34}, \\ \dot{\mathcal{G}}_{34} &= -i(\Delta_s - \Delta_c)\mathcal{G}_{34} - \Gamma_{34}(\mathcal{G}_{33} + \mathcal{G}_{44}) - (\Gamma_3 + \Gamma_4)\mathcal{G}_{34} - \frac{i}{2}(\Omega_s\mathcal{G}_{32} - \Omega_p\mathcal{G}_{14} - \Omega_c\mathcal{G}_{24}),\end{aligned}\tag{13}$$

and the other elements not included in Eq. (13) satisfy the complex conjugate relation: $\mathcal{G}_{ij} = \mathcal{G}_{ji}^*$.

The results of the GKE for weak probe field are shown in Figs. 3, 4, and 5.

In Fig. 3, we show the EIT and the GKE in this system. Panels (a) and (c) are absorption line shapes I_p , panels (b) and (d) are Q_p parameter. The blue and red crosses are the experimental results of Ref. [12], the solid lines and dashed-dot lines are our theoretical results. The experiment of Ref. [12] is carried out in a vapor-cell magneto-optic trap (MOT). The trapped Rb atom clouds is about 1mm in diameter and contains about 2×10^7 Rb atoms. The Rb atom vapor pressure is about 10^{-8} Torr. In the experiment of Ref. [12], there is no effect of SGC, that is, the SGC factor $\beta = 0$. As shown in the figure, our theoretical results and experimental results are in agreement well [69]. Fig. 3 (a) and (b) show the standard EIT signal when the switching field is turned off. As the Rabi frequency Ω_c increases from 11MHz to 24MHz, the absorption line shape I_p and Q_p spectra show the power broaden, which reflects the influence of the strengths of the coupling filed. The behavior of the photon emission at resonance shows anti-bunching. In contrast, when the EIT occurs at $\Delta_p = 0$, the behavior of photon emission

shows bunching. And, there is the sharp “hole” in Q_p spectra which is shown in the inset of Fig. 3 (b). The reason for this “hole” is that the photon emission stops once the dark state is formed [43, 49].

When the switching field Ω_s is turn-on, there is absorption at $\Delta_p = 0$ as shown in Fig. 3 (c). The two absorption sidebands are the usual Aulter-Townes (AT) doublets, and the central peak is the Kerr nonlinear absorption. There is no “hole” on the Q_p spectra since the EIT is destroyed in this process. We show Q_p parameter for the strengths of probe field $\Omega_p = 15\text{MHz}$ by using dashed green line in Fig. 3 (d). This result is not the same with those under the usual condition where anti-bunching behavior can not be captured as the strengths of the probe field increases [43, 49]. And the anti-bunching behavior of photon emission holds on as the strengths of the probe field Ω_p increases. In other words, the strengths of the probe field can not change the anti-bunching behavior. This stable anti-bunching behavior of photon emission demonstrates the ability of photon switching, and that the N -type system based on the GKE can serve as the few photon emitter [70].

Furthermore, we show the absorption line shapes I_p (panels (a) and (c)) and Q_p parameter (panels (b) and

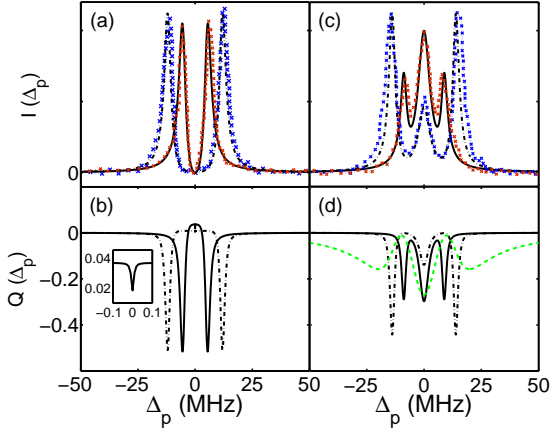


FIG. 3: (Color online) The absorption line shapes I_p (panels (a) and (c)) and Mandel's Q_p parameter (panels (b) and (d)) of the N -type system. Panels (a) and (b) is for the switching field turn-off, panels (c) and (d) is for the switching field turn-on, $\Omega_s = 14$ MHz. The blue and red crosses are the experimental results in Fig. 3 of Ref. [12]. The inset shows the fine structure of the hole on the Q_p spectra for the solid line around $\Delta_p = 0$. The parameters are $\gamma_{31} = \gamma_{32} = 1.4375$ MHz, $\gamma_{41} = \gamma_{42} = 1.5167$ MHz. $\Delta_c = \Delta_s = 0$, and $\beta = 0$. $\Omega_p = 1.5$ MHz, $\Omega_c = 11$ MHz (solid lines), $\Omega_c = 24$ MHz (dashed-dot lines). The initial condition is $|\psi\rangle = |1\rangle$. The dashed green line of Mandel's Q_p parameter is under the conditions of $\Omega_p = 15$ MHz, $\Omega_c = 24$ MHz, $\Omega_s = 14$ MHz.

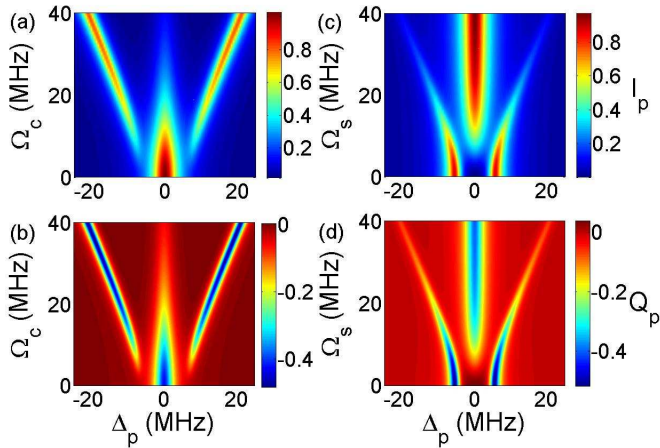


FIG. 4: (Color online) The absorption line shapes I_p (panels (a) and (c)) and Mandel's Q_p parameter (panels (b) and (d)) of the N -type system as the functions of Rabi frequencies Ω_c (panels (a) and (b)), Ω_s (panels (c) and (d)) and detuning frequency Δ_p . The parameters are $\Omega_p = 1.5$ MHz, $\Omega_s = 14$ MHz (panels (a) and (b)); $\Omega_p = 1.5$ MHz, $\Omega_c = 11$ MHz (panels (c) and (d)). The other parameters are the same with Fig. 3.

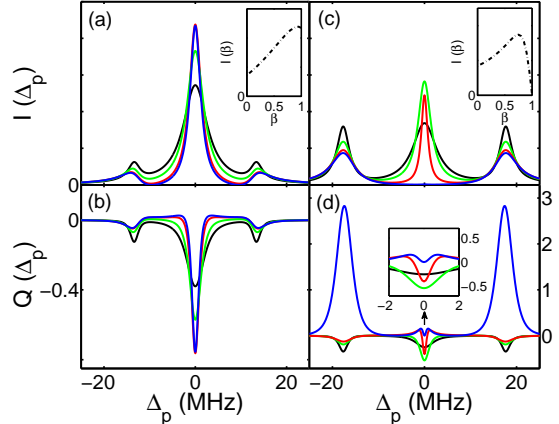


FIG. 5: (Color online) The absorption line shapes I_p (panels (a) and (c)) and Mandel's Q_p parameter (panels (b) and (d)) of the N -type system. $\Omega_p = 1.5$ MHz, $\Omega_s = 25$ MHz, $\Omega_c = 10$ MHz (panels (a) and (b)), 25MHz (panels (c) and (d)). The SGC factor $\beta = 0$ (black line), $\beta = 0.5$ (green line), $\beta = 0.9$ (red line), $\beta = 1$ (blue line). The other parameters are the same with Fig. 3. The insets in panels (a) and (c) show the height of the Kerr nonlinear absorption peak of line shapes as the function of β , the inset in panel (d) shows Mandel's Q_p parameter near resonance $\Delta_p = 0$.

(d)) as the function of Rabi frequencies Ω_c (panels (a) and (b)), and Ω_s (panels (c) and (d)) in Fig. 4. It shows that the strengths of the driven fields play an important role in the GKE. They can control the nonlinearity and the AT splitting.

As shown in Fig. 4 (a) there is mainly one central peak for the absorption line shapes at $\Delta_p = 0$ for small Ω_c , corresponding to the one-photon process $|3\rangle \rightarrow |1\rangle$. From the view of dressed state theory [12, 16], the coupling field with “pure” state $|3\rangle$ induce a pair of dressed states $|-\rangle$ and $|+\rangle$ (instead of state $|3\rangle$). The transitions from states $|1\rangle$ to $|-\rangle$ and $|+\rangle$ are probed by the probe field Ω_p , the transitions from states $|-\rangle$ and $|+\rangle$ to $|4\rangle$ are pumped by the switching field Ω_s . The separation between states $|-\rangle$ and $|+\rangle$ are controlled via the coupling field. When $\Delta_c = 0$, the two dressed states are equally driven, the height of AT doublets are the same. As the Rabi frequency Ω_c increases, the one-photon process is weakened, that is, the interference between the transitions $|-\rangle \rightarrow |1\rangle$ and $|+\rangle \rightarrow |1\rangle$ is destructive. In contrast, the two-photon processes $|4\rangle \rightarrow |-\rangle \rightarrow |1\rangle$ and $|4\rangle \rightarrow |+\rangle \rightarrow |1\rangle$ are being enhanced, and the height of AT doublets at sidebands gets bigger.

For small Ω_s there is only AT doublets of absorption line shapes I_p , this is not the same with the above case. It is shown in Fig. 4 (c). Under this condition, the Kerr nonlinearity is trivial, which can also be realized for far off resonance of the switching field. As Ω_s increases, however, the central peak at $\Delta_p = 0$ increases nonlinearly until its steady value. Physically, this nonlinear increase is determined by the strengths of the coupling field Ω_c ,

and the steady process of I_p is related to the probe field. Another influence of switching field is, the splitting of the AT doublets gets bigger when Ω_s increases. The reason is that the splitting between the dressed states can also be affected by the switching field Ω_s , this splitting is $\propto \sqrt{\Omega_c^2 + \Omega_s^2}$. Our numerical results verify this behavior.

In Fig. 4 (b) and (d) we show the spectra of Mandel's Q_p parameters. For the central Kerr absorption at $\Delta_p = 0$, one can see magnitude of Q_p parameters decreases with Ω_c and increases with Ω_s . The reason is that the coupling field can inhibit the Kerr absorption process, while the switching field can enhance it. However, Q_p parameters stay minus at resonance, which means the strengths of the coupling field Ω_c or the switching field Ω_s can not change the natures of the photon statistics: the anti-bunching or the bunching.

In the above consideration we do not include the effect of SGC. In fact, it is also possible to introduce the effect of SGC into the nonlinear Kerr absorption. The results for different SGC factor β are shown in Fig. 5. The top row is absorption line shapes I_p , and the bottom row is Q_p parameter.

To better show GKE, we chose the parameters to make the one-photon process obvious. In Fig. 5 (a) and (b), we show the results of $\Omega_s = 25\text{MHz}$, $\Omega_c = 10\text{MHz}$. We can see from the figure, the Kerr absorption is more obvious than that of AT doublets. As the SGC factor β increases (from 0 to 1), the AT doublets are being restrained. The central Kerr peak, however, is “coherently narrowed and enhanced” (see Fig. 5 (a)). The behavior of the Kerr absorption shows nonlinear change with the increasing of β , as shown in the inset of Fig. 5 (a). The values of Q_p parameters (panel (b)) become negative big at $\Delta_p = 0$ as β increases, which means that the anti-bunching effect becomes more obvious. Also, Q_p spectra becomes narrow around $\Delta_p = 0$.

We further consider another special case: $\Omega_c = \Omega_s = 25\text{MHz}$. The results are shown in Fig. 5 (c) and (d). We see that the separation of the AT doublets increases to 35.36MHz . The Kerr absorption peak as the function of β is shown in the inset of Fig. 5 (c). Its behavior in this case is different with that of the above case. What is particular in this case is the central Kerr absorption goes to zero when $\beta = 1$. That is, the nonlinear Kerr absorption is eliminated due to SGC, it is shown as the blue line in Fig. 5 (c). This can also be viewed as the retrieval of dark state in the system. The reason is that there exists the quantum interference between the one-photon and two-photon processes for $\beta = 1$. For $\beta = 0$, however, there is no this quantum interference. In addition, the behavior of photon emission is affected by SGC: Q_p parameter changes from negative to positive values when β gets

big, which is different with the above case. The inset in panel (d) shows this change at the detuning $\Delta_p = 0$.

IV. BRIEF CONCLUSION

In this work we investigate the effects of SGC on the electromagnetically induced transparency (EIT) and the giant Kerr effect (GKE) of four-level quantum system of the ^{87}Rb atom driven by external cw laser fields.

In our study, we show the structure of absorption line shapes in the detuning space for the double Λ -type system. The usual EIT means that we can control the quantum system (such as the ^{87}Rb atom) by employing the strong coupling field, and there is no absorption when the weak probe field is introduced under the condition of two-photon resonance. With the effect of SGC, there exist new EIT channels, we note them as the “vacuum-assisted transparency” (VAT). It means that we can use external fields to lock the system, so that there is no absorption when the probe field is introduced even beyond the two-photon resonance condition. The transparency window crosses the whole detuning range of the probe field. Also, this could be more convenient to operate in experiment than the usual EIT setup.

The coupling field Ω_c and the switching field Ω_s play the different role in GKE for the N -type system: the former one can inhibit the nonlinear absorption, while the later one can enhance it. If there exists SGC in the system, the nonlinear Kerr absorption can be either narrowed or eliminated under different driven conditions. When the nonlinear absorption is completely eliminated, the dark state can be repaired by SGC.

For the photon statistics, several kinds of behaviors of Mandel's Q parameter, such as the “hole” of the dark state, the steady anti-bunching of the photon switching, the transition between bunching and anti-bunching near resonance, and the big fluctuation due to SGC are also studied.

Based on this work, the dynamics of other type four level systems, such as the Y -type, the inverse Y -type systems can be investigated. Also, this study will be of interest for further investigation in few photon processes, spontaneous emission cancellation, etc.

Acknowledgments

We thank the referee for a helpful comments. This work was supported by the National Science Foundation of China (Grant No. 91021009, 10874102), and National Basic Research Program of China (973 Program, Grant No. 2009CB929404).

[1] K. J. Boller, A. Imamoglu, and S. E. Harris, Phys. Rev. Lett. **66**, 2593 (1991).

[2] S. E. Harris, Phys. Today **50**, No. 7, 36 (1997).

[3] A. J. Merriam, S. J. Sharpe, M. Shverdin, D. Manuszak,

G. Y. Yin, and S. E. Harris, Phys. Rev. Lett. **84**, 5308 (2000).

[4] M. Fleischhauer, A. Imamoglu, and J. P. Marangos, Rev. Mod. Phys. **77**, 633 (2005).

[5] Y. D. Chong and M. Soljacic, Phys. Rev. A **77**, 013823 (2008).

[6] A. Lezama, S. Barreiro, and A. M. Akulshin, Phys. Rev. A **59**, 4732 (1999).

[7] Y. Zhang, A. W. Brown, and M. Xiao, Phys. Rev. Lett. **99**, 123603 (2007).

[8] C. Butch, R. Santra, and L. Young, Phys. Rev. Lett. **98**, 253001 (2007).

[9] A. A. Abdumalikov, Jr., O. Astafiev, A. M. Zagoskin, Y. A. Pashkin, Y. Nakamura, and J. S. Tsai, Phys. Rev. Lett. **104**, 193601 (2010).

[10] H. Schmidt and A. Imamoglu, Opt. Lett. **21**, 1936 (1996).

[11] A. Imamoglu, H. Schmidt, G. Woods, and M. Deutsch, Phys. Rev. Lett. **79**, 1467 (1997).

[12] M. Yin, E. G. Rickey, and Y. Zhu, Opt. Lett. **26**, 548 (2001).

[13] M. Yan, E. G. Rickey, and Y. Zhu, Phys. Rev. A **64**, 041801(R) (2001).

[14] H. Kang and Y. Zhu, Phys. Rev. Lett. **91**, 093601 (2003).

[15] D. A. Braje, V. Balic, G. Y. Yin, and S. E. Harris, Phys. Rev. A **68**, 041801(R) (2003).

[16] W. Xu and J. Gao, Phys. Rev. A **67**, 033816 (2003).

[17] S. Li, X. Yang, X. Cao, C. Zhang, C. Xie, and H. Wang, Phys. Rev. Lett. **101**, 073602 (2008).

[18] M. Bajcsy, S. Hofferberth, V. Balic, T. Peyronel, M. Hafezi, A. S. Zibrov, V. Vuletic, and M. D. Lukin, Phys. Rev. Lett. **102**, 203902 (2009).

[19] Y. Niu and S. Gong, Phys. Rev. A **73**, 053811 (2006).

[20] W. Jiang, X. Yan, J. Song, H. Zheng, C. Wu, B. Yin, and Y. Zhang, Opt. Commun. **282**, 101 (2009).

[21] G. F. Sinclair and N. Korolkova, Phys. Rev. A **76**, 033803 (2007); **77**, 033843 (2008).

[22] G. F. Sinclair, Phys. Rev. A **79**, 023815 (2009).

[23] M. J. Hartmann and M. B. Plenio, Phys. Rev. Lett. **99**, 103601 (2007).

[24] S. Rebić, J. Twamley, and G. J. Milburn, Phys. Rev. Lett. **103**, 150503 (2009).

[25] X. Yang and S. Zhu, Phys. Rev. A **77**, 063822 (2008).

[26] M. Xie and G. Yang, Opt. Commun. **282**, 1819 (2009).

[27] A. K. Patnaik and G. S. Agarwal, J. Mod. Opt. **45**, 2131 (1998).

[28] A. K. Patnaik and G. S. Agarwal, Phys. Rev. A **59**, 3015 (1999).

[29] P. R. Berman, Phys. Rev. A **58**, 4886 (1998).

[30] G. S. Agarwal and P. K. Pathak, Phys. Rev. A **70**, 025802 (2004).

[31] Z. Ficek and S. Swain, Phys. Rev. A **69**, 023401 (2004).

[32] J. H. Li, J. B. Liu, A. X. Chen, and C. C. Qi, Phys. Rev. A **74**, 033816 (2006).

[33] C. Wang, A. Li, X. Zhou, Z. Kang, J. Yun, and J. Gao, Opt. Lett. **33**, 687 (2008).

[34] C. Wang, Z. Kang, S. Tian, J. Yun, and J. Gao, Phys. Rev. A **79**, 043810 (2009).

[35] H. R. Xia, C. Y. Ye, and S. Y. Zhu, Phys. Rev. Lett. **77**, 1032 (1996).

[36] L. Li, X. Wang, J. Yang, G. Lazarov, J. Qi, and A. M. Lyyra, Phys. Rev. Lett. **84**, 4016 (2000).

[37] D. G. Norris, L. A. Orozco, P. Barberis-Blostein, and H. J. Carmichael, Phys. Rev. Lett. **105**, 123602 (2010).

[38] Y. Zheng and F. L. H. Brown, Phys. Rev. Lett. **90**, 238305 (2003).

[39] Y. Zheng and F. L. H. Brown, J. Chem. Phys. **119**, 11814 (2003).

[40] S. Mukamel, Phys. Rev. A **68**, 063821 (2003).

[41] Y. He and E. Barkai, Phys. Rev. Lett. **93**, 068302 (2004).

[42] G. Bel, Y. Zheng and F. L. H. Brown, J. Phys. Chem. B **110**, 19066 (2006).

[43] Y. Peng, Y. Zheng, and F. L. H. Brown, J. Chem. Phys. **126**, 104303 (2007).

[44] Y. Peng, S. Xie, Y. Zheng and F. L. H. Brown, J. Chem. Phys. **131**, 214107 (2009).

[45] Y. Peng, Y. Zheng, Phys. Rev. A **80**, 043831 (2009).

[46] B. Han and Y. Zheng, Phys. Rev. A **78**, 015402 (2008).

[47] B. Han, Z. Ji, and Y. Zheng, J. Chem. Phys. **130**, 244502 (2009).

[48] Y. Peng, D. Wang, Y. Zheng, and S. Xie, Physica E **42**, 2242 (2010).

[49] D. Wang and Y. Zheng, Chin. Phys. B **19**, 083202 (2010).

[50] G. S. Agarwal, *Quantum Statistical Theories of Spontaneous Emission and Their Relation to Other Approaches*, edited by G. Mohler *et al.* Springer Tracts in Modern Physics: Quantum Optics Vol. **70** (Springer-Verlag, Berlin, 1974), Sec. 15.

[51] D. A. Cardimona, M. G. Raymer, and C. R. Stroud, Jr., J. Phys. B **15**, 55 (1982).

[52] D. A. Cardimona and C. R. Stroud, Jr., Phys. Rev. A **27**, 2456 (1983).

[53] M. Fleischhauer and M. D. Lukin, Phys. Rev. Lett. **84**, 5094 (2000).

[54] J. Javanainen, Europhys. Lett. **17**, 407 (1992).

[55] S. Y. Zhu and M. O. Scully, Phys. Rev. Lett. **76**, 388 (1996).

[56] S. Menon and G. S. Agarwal, Phys. Rev. A **57**, 4014 (1998).

[57] B. W. Shore and K. Bergmann, Rev. Mod. Phys. **70**, 1003 (1998).

[58] S. Zhu, Phys. Rev. Lett. **76**, 388 (1996).

[59] E. Paspalakis and P. L. Knight, Phys. Rev. Lett. **81**, 293 (1998).

[60] P. Zhou and S. Swain, Phys. Rev. Lett. **77**, 3995 (1996).

[61] P. Zhou and S. Swain, Phys. Rev. Lett. **78**, 832 (1997).

[62] F. Carreño, O. G. Calderón, M. A. Antón, and I. Gonzalo, Phys. Rev. A **71**, 063805 (2005).

[63] M. A. Antón, O. G. Calderón, and F. Carreño, Phys. Rev. A **72**, 023809 (2005).

[64] I. Gonzalo, M. A. Antón, F. Carreño, and O. G. Calderón, Phys. Rev. A **72**, 033809 (2005).

[65] K. Blum, *Density Matrix Theory and Applications*, 2ed ed. (Plenum, New York, 1981).

[66] C. Tannoudji, J. Dupont Roc, and G. Grynberg, *Atom -Photon Interactions* (Wiley Interscience, New York, 1992).

[67] P. W. Milonni and W. A. Smith, Phys. Rev. A **11**, 814 (1975).

[68] L. Mandel and E. Wolf, *Optical Coherence and Quantum Optics*, (Cambridge University Press, New York, 1995).

[69] The tiny departure is mainly due to the atom collision and finite laser linewidths in practice as pointed out in Ref. [12].

[70] A. Imamoglu, Phys. Rev. Lett. **89**, 163602 (2002).

[71] D. A. Steck, *Rubidium 87 D Line Data*, available online at <http://steck.us/alkalidata> (revision 2.1.2, 12 August 2009).

[72] M. Maric, J. J. McFerran, and A. N. Luiten, Phys. Rev.

A **77**, 032502 (2008).
[73] D. Aumiler, T. Ban, and G. Pichler, Phys. Rev. A **79**, 063403 (2009).